Cellular Microbiology (2013) doi:10.1111/cmi.12121

VEGF receptor-1 involvement in pericyte loss induced by *Escherichia coli* in an *in vitro* model of blood brain barrier

Mario Salmeri,[1†] Carla Motta,[2†] Carmelina D. Anfuso,[2] Andrea Amodeo,[1] Marina Scalia,[3] Maria A. Toscano,[1] Mario Alberghina[2] and Gabriella Lupo[2*]

[1]*Department of Bio-medical Sciences, University of Catania, Catania, Italy.*

[2]*Department of Clinical and Molecular Biomedicine, University of Catania, Catania, Italy.*

[3]*Department G.F. Ingrassia, Unit of General and Cellular Biology and Molecular Genetics 'G.Sichel', University of Catania, Catania, Italy.*

Summary

The key aspect of neonatal meningitis is related to the ability of pathogens to invade the blood–brain barrier (BBB) and to penetrate the central nervous system. In the present study we show that, in an *in vitro* model of BBB, on the basis of co-culturing primary bovine brain endothelial cells (BBEC) and primary bovine retinal pericytes (BRPC), *Escherichia coli* infection determines changes of transendothelial electrical resistance (TEER) and permeability (Pe) to sodium fluorescein. In the co-culture model, within BBEC, bacteria are able to stimulate cytosolic and Ca^{2+}-independent phospholipase A_2 ($cPLA_2$ and $iPLA_2$) enzyme activities. In supernatants of *E. coli*-stimulated co-cultures, an increase in prostaglandins (PGE_2) and VEGF production in comparison with untreated co-cultures were found. Incubation with *E. coli* in presence of $AACOCF_3$ or BEL caused a decrease of PGE_2 and VEGF release. SEM and TEM images of BBEC and BRPC showed *E. coli* adhesion to BBEC and BRPC but only in BBEC the invasion occurs. VEGFR-1 but not VEGFR-2 blockade by the specific antibody reduced *E. coli* invasion in BBEC. In our model of BBB infection, a significant loss of BRPC was observed. Following VEGFR-1, but not VEGFR-2 blockade, or in presence of $AACOCF_3$ or BEL, elevated TEER values, reduced permeability and BRPC loss were found. These data suggest that VEGFR-1 negatively regulates BRPC survival and its blockade protects the barrier integrity. PGs and VEGF could exert a biological effect on BBB, probably by BRPC coverage ablation, thus increasing BBB permeability. Our results show the role played by the BBEC as well as BRPC during a bacterial attack on BBB. A better understanding of the mechanisms by which *E. coli* enter the nervous system and how bacteria alter the communication between endothelial cells and pericytes may provide exciting new insight for clinical intervention.

Received 6 July, 2012; revised 4 February, 2013; accepted 6 February, 2013. *For correspondence. E-mail lupogab@unict.it; Tel. (+39) 95 7384252/7384071; Fax (+39) 95 7384220.
†These authors contributed equally.

Introduction

Through the years, bacterial meningitis has remained an infection with a high mortality rate, particularly in very young and elderly patients, despite advances in antimicrobial therapy (Kim, 2003; 2008). The reason for the poor outcome has been attributed to limited knowledge of pathogenesis and pathophysiology of the disease. Although most cases of *Escherichia coli* meningitis occur via haematogenous spread, it is not yet clear what microbial and host factors are responsible for the ability of neurotropic strains of *E. coli* to cross the blood–brain barrier (BBB). The bacterium itself or its degraded products stimulate the release of pro-inflammatory mediators such as cytokines and prostaglandins (PGs) by leucocytes, endothelial cells (EC), astrocytes, microglial cells and other cells in the central nervous system (CNS), and these subsequently lead to an increase in the permeability of the BBB (Engblom *et al.*, 2002; Zhu *et al.*, 2010a).

The BBB is an active interface between the circulation and the CNS which restricts the free movement of different substances between the two compartments and plays a crucial role in the maintenance of the homeostasis of the CNS. The principal components of the BBB are the EC, astrocytes and pericytes (PC) (Fig. 1A). Some other cellular elements like neurones or microglia, components of the neurovascular unit, play also a significant role in the function of BBB (Stanimirovic and Friedman, 2012). From the point of view of the permeability the most important

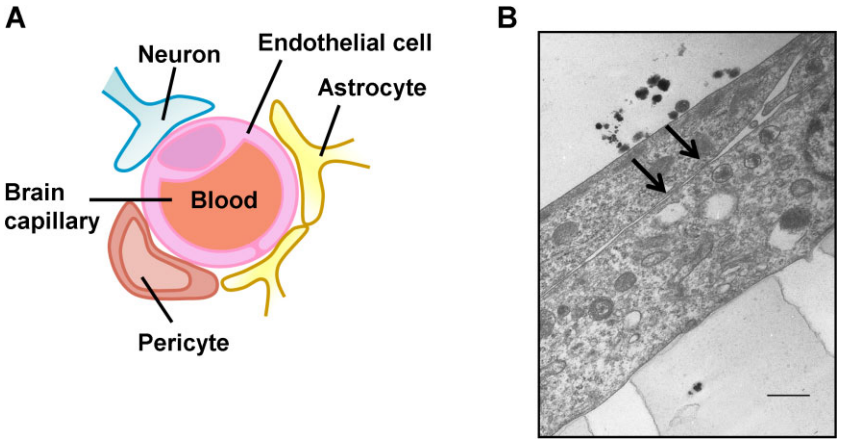

Fig. 1. Schematic drawing of neurovascular unit (A) and transmission electron micrographs (B) of bovine brain microvascular endothelial cells (BBEC). Two elongated primary BBEC cultured onto the Transwell membranes display typical morphology of the endothelial cells. The black arrows (B) indicate the tight junctional elements between two primary BBEC. Bar equals to 200 nm.

cell types of the BBB are cerebral EC which form a continuous sheet covering the inner surface of the capillaries. EC are interconnected by tight junctions (TJ), (Fig. 1B) crucial in determining alterations in the control of BBB vascular permeability (Nico and Ribatti, 2012). The transcellular entry of *E. coli* K1 through human brain microvascular endothelial cells (HBMEC) is responsible for TJ disruption and it has demonstrated the involvement of IQGAP1 (Ras GTPase-activating-like protein) in promoting *E. coli* K1 invasion of brain EC (Krishnan *et al.*, 2012).

Brain EC have both endothelial-like features (i.e. expression of von Willebrand factor) and epithelial-like features such as low level of pinocytosis and high transendothelial electrical resistance (TEER). EC sit on the basal membrane which consists mainly of collagen IV, fibronectin, laminin and proteoglycans. Engulfed in the basal membrane are the PC, which cover approximately 22–32% of the endothelium. PC are uniquely positioned within the neurovascular unit to serve as vital integrators, co-ordinators and effectors of many neurovascular functions, including angiogenesis, BBB formation and maintenance, vascular stability and angio-architecture and regulation of capillary blood flow (Armulik *et al.*, 2010; Winkler *et al.*, 2011). These cells are also seen as multipotent cells and so with great potential for therapy (Dore-Duffy, 2008).

New studies have revealed that PC deficiency in the CNS leads to BBB breakdown and brain hypoperfusion resulting in secondary neurodegenerative changes (Sá-Pereira *et al.*, 2012).

Do the PC have a role in *E. coli* crossing the BBB? Certainly the PC provide a structural barrier that helps to promote vascular integrity and the pericytal dysfunction or the loss of PC could play an important role in the pathogenesis of meningitis. The role of PC in maintenance of BBB during bacterial meningitis is still to be elucidated. Our study places the vital cross-talk between EC and PC at the centre of injury responses in bacterial meningitis.

Arachidonate metabolites such as PGs and leukotrienes (LTs) contribute to *E. coli* K1 invasion of microvascular EC and penetration into the brain (Zhu *et al.*, 2010a,b). Arachidonic acid (AA) is liberated from phospholipids by the action of different isoforms of phospholipases (PLA_2s) and converted to PGs or LTs by the action of cyclooxygenase (COX) and 5-lipoxygenase respectively. Cytosolic PLA_2 ($cPLA_2$), Ca^{2+}-independent intracellular PLA_2 ($iPLA_2$) and Ca^{2+}-dependent secretory PLA_2 ($sPLA_2$) differ from each other in terms of substrate specificity, Ca^{2+} requirement, lipid modification, translocation to cellular membranes and AA release (Alberghina, 2010). $cPLA_2$ and $iPLA_2$ are ubiquitously present and active in mammalian cells, whereas $sPLA_2$ may be silent or not expressed in quiescent EC. Our previous study has shown the role of $cPLA_2$, $iPLA_2$ and PKCα/ERK/MAPK signalling pathways in governing the *E. coli* penetration into the BBEC (Salmeri *et al.*, 2012), but how those signalling molecules contribute to the invasion is still to be completely understood.

The vascular endothelial growth factor (VEGF) is a crucial regulator of vasculogenesis, angiogenesis, lymphangiogenesis and vascular permeability in vertebrates (Kajdaniuk *et al.*, 2011). VEGF-A, the prototype VEGF ligand, binds and activates two tyrosine kinase receptors: VEGFR-1 (Flt-1) and VEGFR-2 (KDR/Flk-1). The transmembrane VEGFR-1 acts as a positive regulator of angiogenesis, inflammatory responses and permeability in several human diseases such as rheumatoid arthritis (Kong *et al.*, 2011), cancer (Subramanian *et al.*, 2010) and bacterial meningitis with *E. coli* playing a role in the promotion of the physical association between phosphorylated VEGFR-1 and p85 subunit of PI3K, highlighting the involvement of VEGFR-1 in *E. coli* K1 invasion of microvascular ECs (Zhao *et al.*, 2010).

High VEGF levels have been measured in the cerebrospinal fluid (CSF) of patients with bacterial meningitis who show severe BBB disruption, and VEGF immunoreactivity was found in endothelium and smooth-muscle cells from brain specimens of patients who died of bacterial meningitis (van der Flier *et al*., 2001).

Of particular interest are the results reported by J.I. Greeberg *et al*., demonstrating the VEGF as an inhibitor of neovascularization based on its capacity to disrupt the vascular smooth muscle cells function; specifically, VEGF ablates PC coverage of nascent vascular sprouts leading to vessel destabilization (Greenberg *et al*., 2008). It has been demonstrated that VEGF can stimulate PGI_2 synthesis via $cPLA_2$-mediated AA release, indicating that VEGF stimulation of this biosynthetic pathway may occur, at least in part, via activation of p42/p44 MAP kinases (Wheeler-Jones *et al*., 1997) and that activation of PKC plays a crucial role in this VEGF signalling, suggesting that the PKC delta isoform may be a key mediator of VEGF-induced activation of the ERK pathway via increased association with Raf-1 (Gliki *et al*., 2001).

In the present article we show that, in an *in vitro* model of BBB, on the basis of co-culturing BBEC and BRPC, *E. coli* invasion is associated with decreased TEER and increased permeability of the BBB due to the loss of PC. Furthermore we present evidence that pericytal VEGFR-1 plays a significative role in these events. These findings suggest a possible mechanism by which EC and PC react to the *E. coli* infection.

Results

E. coli *infection determines changes of TEER and permeability to sodium fluorescein in BBEC/BRPC co-cultures*

The interaction among the cells forming the neurovascular unit is shown in a schematic drawing in Fig. 1A. TEM of BBEC growing on Transwell filter in the BBB model is shown in Fig. 1B. TJ sealing the BBEC are evident.

The BBB model used in the present study is shown in Fig. 2. To highlight the cell phenotype, and for immunological characterization, subconfluent BBEC were incubated with anti-von Willebrand factor rabbit polyclonal antibody (BBEC marker, Fig. 2A) and BRPC with mouse monoclonal against α-actin (BRPC marker, Fig. 2B): the distribution of immunocomplexes, observed by confocal immunofluorescence microscopy, showed an elongated and spindle shape for BBEC and an irregular, large and stellate shape for BRPC. Images in Fig. 2A and B are not of the true BBB model, but rather an approximation using subconfluent cells.

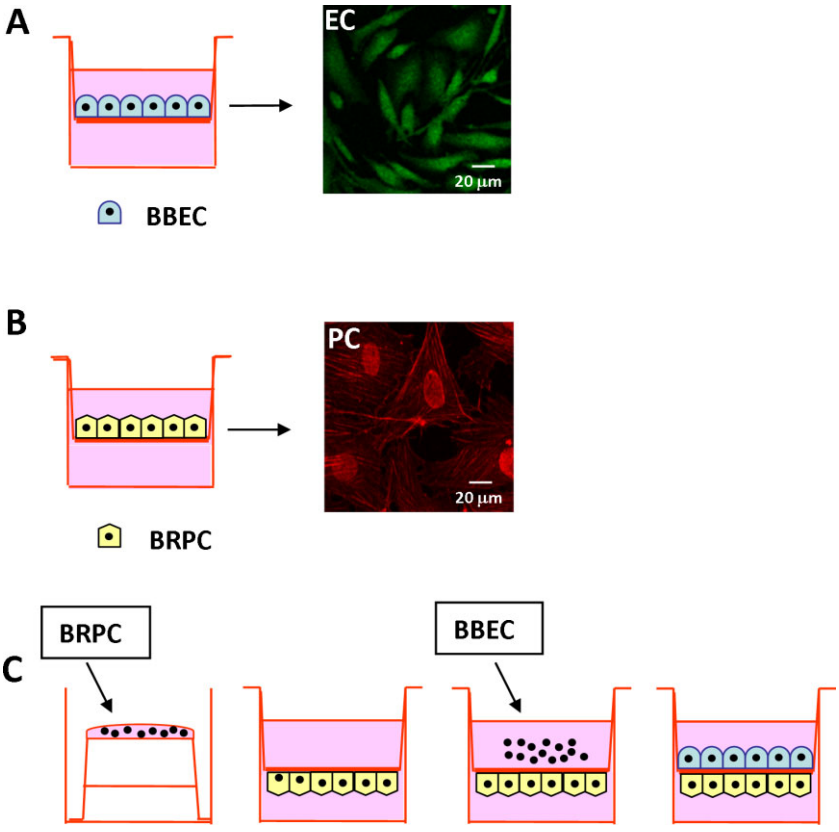

Fig. 2. Scheme of Transwell systems for mono- and co-cultures of bovine brain endothelial cells (BBEC) and bovine retinal pericytes (BRPC). (A) BBEC monolayers. (B) BRPC monolayers. (C) BRPC were seeded on the lower side of the membrane until confluence, and then the BBEC were seeded in the upper compartment. The pore size of 3.0 μm was chosen to allow the passage of cell foot processes through the membrane filter separating the upper and lower chamber. The pore size of 0.4 μm was chosen for the experiments in which the cells were trypsinized and counted. Images of control BBEC or BRPC are shown in (A) and (B). To highlight cells architecture and for immunological characterization, BBEC non-confluent monolayers were washed, fixed, permeabilized and stained with a polyclonal anti-von Willebrand factor (vWF) antibody, coupled to a green fluorescent-labelled secondary antibody, and BRPC were stained with a monoclonal anti-α actin antibody coupled to a red fluorescent-labelled secondary antibody. Distribution of immunocomplexes was observed by confocal immunofluorescence microscopy. Magnification 40 ×.

Table 1. Evaluation of the barrier integrity.

		TEER ($\omega \times cm^2$)	Pe (10^{-6} cm s^{-1})
Mono-culture	BBEC	78 ± 11.2	8.1 ± 0.6
	BBEC + *E. coli*	66 ± 8.4	6.6 ± 0.8
Co-culture	BBEC/BRPC	267 ± 22.1[a]	3.2 ± 0.15[a]
	BBEC/BRPC + *E. coli*	83 ± 9.1[b]	7.3 ± 0.5[b]

a. A statistically significant difference between uninfected BBEC and BBEC/BPRC cultures.
b. A statistically significant difference between uninfected and infected BBEC/BPRC co-cultures.
BBEC (40 000 cells cm^{-2}) were cultured in monolayers in Ham's F-10 medium containing 10% FBS or were grown on the top surface of the Transwell insert (six-well type, 3.0 μm pore size) in which BRPC (40 000 cells cm^{-2}) were first plated on the outside of the membrane, in 50% DMEM plus 50% F-10 HAM's containing 10% FBS. After 3 days, the cells were incubated in absence or presence of *E. coli* (10^7 cfu per well) for 60 min and measurements of TEER and cell permeability on BBEC were performed as described in *Experimental procedures*. For TEER measurements, the collagen-treated Transwell inserts were used to measure the background resistance. Values (means ± SEM) are from six independent experiments ($n = 6$), were expressed as $\omega \times cm^2$ and were calculated by the formula: [the average resistance of experimental wells – the average resistance of blank cells] × 0.33 (the area of the Transwell membrane).
For sodium fluorescein determination, flux across cell-free inserts was measured and transendothelial permeability coefficient (Pe) was calculated. Values (means ± SEM) are from three independent experiments ($n = 3$). ANOVA and the Tukey post-test were used to compare TEER or permeability measurements in the four different experimental conditions ($P < 0.05$).
TEER and permeability to sodium fluorescein (Pe) determination in microvascular endothelial cells in mono- and in co-culture, in the absence or presence of *E. coli* K1 strain.

The BBB model, used in all experiments with confluent cells, was characterized by measuring TEER and sodium fluorescein flux across BBEC in monolayer and in co-culture with BRPC (Table 1). Co-culture showed high values of TEER and very low permeability to sodium fluorescein in comparison with BBEC mono-culture. Very similar results in repeated experiments indicated the reproducibility of the model. Incubation for 60 min with *E. coli* K1 (10^7 cfu per well) caused a significant TEER reduction (about 3.2-fold) and an increased permeability (about 2.3-fold) as compared with BBEC/BRPC control co-cultures.

E. coli *stimulates phospholipase A_2 activities, PGE_2 production and VEGF release*

As reported in Table 2, in *E. coli*-stimulated BBEC in mono- and co-culture, PLA_2 activity was strongly activated (about 2.2-fold in mono- and 2.6-fold in co-cultures) compared with the control (unstimulated) BBEC, unlike BRPC in which it was weakly stimulated. In control BBEC mono-cultures, the presence for 120 min (pre-incubation of 60 min followed by incubation for 60 min in the presence of bacteria) of 50 μM $AACOCF_3$ (PLA_2 activity dual blocker) or 2.5 μM BEL ($iPLA_2$ inhibitor) caused a

Table 2. PLA_2 activity in BBEC and BRPC in mono- and co-culture stimulated and non-stimulated by *E. coli* K1.

		PLA_2 activity (pmol min^{-1} mg^{-1})	
		Control cells	Cells + *E. coli*
Mono-culture	BBEC	19.9 ± 1.5	44.7 ± 3.2*
	BBEC + $AACOCF_3$	14.4 ± 1.1†	17.1 ± 1.5†
	BBEC + BEL	16.1 ± 1.3	20.0 ± 1.7†
	BRPC	13.5 ± 1.1	17.1 ± 1.3
	BRPC + $AACOCF_3$	9.2 ± 0.8†	11.0 ± 1.2†
	BRPC + BEL	10.3 ± 1.2†	12.3 ± 0.9†
Co-culture	BBEC	27.4 ± 2.5	71.2 ± 6.2*
	BBEC + $AACOCF_3$	19.8 ± 1.3†	23.1 ± 2.1†
	BBEC + BEL	22.1 ± 2.2†	31.2 ± 2.4†
	BRPC	12.2 ± 1.1	16.1 ± 1.3
	BRPC + $AACOCF_3$	7.7 ± 0.9	10.3 ± 0.9†
	BRPC + BEL	8.0 ± 1.2	10.2 ± 1.3†

BBEC (40 000 cells cm^{-2}) were cultured in monolayers in Ham's F-10 medium containing 10% FBS or were grown on the top surface of the Transwell insert (six-well type, 3.0 μm pore size) in which BRPC (40 000 cells cm^{-2}) were first plated on the outside of the polycarbonate membrane, in 50% DMEM plus 50% F-10 HAM's containing 10% FBS. All incubations were performed at 37°C in absence or presence of *E. coli* (10^7 cfu per well) for 60 min with or without 50 μM $AACOCF_3$ or 2.5 μM BEL. The incubation with BEL allowed us to discriminate between the $cPLA_2$ and $iPLA_2$ activity contribution. Inhibitors were added to the culture medium 60 min before *E. coli* addition.
PLA_2 activity was measured following enzymatic hydrolysis of arachidonoyl thio-phosphatidylcholine (ATPC). Specific activity in *E. coli* lysates was almost undetectable (data not shown). Values (means ± SEM) are from three independent experiments ($n = 3$). ANOVA and the Tukey post-test were used to compare enzyme activities measurements in the 24 different experimental conditions ($P < 0.05$). Enzyme activities measured in *E. coli*-stimulated BBEC in comparison with control un-stimulated BBEC, are indicated by asterisk (*), and in presence of inhibitors in comparison with the values in absence of inhibitors are indicates by dagger (†). 'Control cells' refers to cells not stimulated by *E. coli*.

Table 3. Prostaglandin (PGE_2) production in BBEC and BRPC in mono- and co-culture stimulated and non-stimulated by *E. coli* K1.

		PGE_2 (pg ml^{-1})	
		Control cells	Cells + *E. coli*
Mono-culture	BBEC	88 ± 7.8	220 ± 21.1*
	BBEC + $AACOCF_3$	73 ± 6.1[a]	82 ± 7.9[a]
	BBEC + BEL	78 ± 6.8[a]	88 ± 8.1[a]
	BRPC	70 ± 6.9	73 ± 6.9[b]
	BRPC + $AACOCF_3$	52 ± 4.8[a]	56 ± 5.1[a]
	BRPC + BEL	57 ± 5.1[a]	59 ± 5.4[a]
Co-culture	BBEC/BRPC	203 ± 19.9[c]	612 ± 46.8[c]*
	BBEC/BRPC + $AACOCF_3$	162 ± 15.8[a]	182 ± 18.8[a]
	BBEC/BRPC + BEL	171 ± 16.5[a]	192 ± 21.1[a]

a. The statistically significant differences in PGE_2 production of cultures incubated with PLA_2 inhibitors in comparison with the respective in absence of inhibitors.
b. The statistically significant differences in PGE2 release in untreated BRPC mono-cultures in comparison with untreated BBEC mono-cultures.
c. The statistically significant differences, between not- and stimulated co-cultures versus the respective mono-cultures.
BBEC (40 000 cells cm^{-2}) were cultured in monolayers in Ham's F-10 medium containing 10% FBS or were grown on the top surface of the Transwell insert (six-well type, 3.0 μm pore size) in which BRPC (40 000 cells cm^{-2}) were first plated on the outside of the polycarbonate membrane, in 50% DMEM plus 50% F-10 HAM's containing 10% FBS. Cell culture supernatants from mono- and co-cultures in absence (control) and presence of *E. coli* (10^7 cfu per well, for 60 min), with or w/o 50 μM $AACOCF_3$ or 2.5 μM BEL, were assayed for PGE_2 production. Inhibitors were added to the culture medium 60 min before *E. coli* addition. Values (means ± SEM) are from three independent experiments ($n = 3$). ANOVA and the Tukey post-test were used to compare PGE_2 production in the 18 different experimental conditions ($P < 0.05$). Stimulated cells versus control cultures (not stimulated by bacteria), are indicated by asterisk (*).

decrease of enzyme activity (28% and 19% respectively); in *E. coli* treated BBEC mono-cultures, $AACOCF_3$ and BEL caused a decrease by 62% and 55% respectively. In control BRPC mono-cultures, PLA_2 activity dual blocker and $iPLA_2$ inhibitor caused a decrease by 32% and 24% respectively, and in *E. coli* stimulated BRPC mono-cultures, the inhibitors caused a decrease by 36% and 28% respectively.

In control BBEC grown in co-culture with BRPC, $AACOCF_3$ reduced enzymatic activity by 28% and BEL by 20% and after *E. coli* treatment in presence of the inhibitors, enzymatic activity decreased by 68% and 56% in BBEC co-cultures. Moreover, the two inhibitors decreased PLA_2 activity in control and in *E. coli* treated BRPC by about 36%. The incubation with BEL allowed us to discriminate between the $cPLA_2$ and $iPLA_2$ activity contribution. The decrease in BBEC enzyme activity in presence of BEL suggests a partial contribution of $iPLA_2$ in mediating AA release of *E. coli*-stimulated cells.

PGE_2 production in supernatants of BBEC or BRPC in mono- and in co-culture was detected. As shown in Table 3, a 2.5-fold increase in BBEC mono-cultures was observed after *E. coli* treatment compared with the respective control (no treatment), and *E. coli* incubation in presence of $AACOCF_3$ (50 μM) or BEL (2.5 μM) decreased PGE_2 production by 63% and 60% respectively. The contribution in PGE_2 production from *E. coli*-treated BRPC mono-cultures was negligible.

PGE_2 production in untreated co-cultures was about 2.6-fold higher than that of the respective mono-cultures; in *E. coli*-treated co-cultures, prostaglandin production was higher than the predicted sum of that produced by BBEC and BRPC mono-cultures. When BBEC/BRPC co-cultures were treated with *E. coli*, the PGE_2 production increased by 3.0-fold in comparison with the respective untreated co-cultures. Furthermore, in the supernatants of *E. coli*-stimulated co-cultures, incubated in presence of PLA_2 inhibitors $AACOCF_3$ or BEL, PGE_2 levels decreased by about 70% and 68% respectively and the decrement was about 20% and 16%, respectively, for untreated co-cultures.

BBEC mono-cultures produced moderate amounts of VEGFA (hereafter referred to as VEGF) protein in the conditioned medium (22.3 ± 1.9) and incubation for 60 min with *E. coli* led to a 3.1-fold increase in the release (Table 4). On the contrary, untreated BRPC mono-cultures expressed VEGF at levels 1.6-fold higher than untreated BBEC mono-cultures and the presence of *E. coli* did not induce any increase in the secretion. Moreover, in the untreated co-cultures, the VEGF amount was greater than the predicted sum of that produced by solo cultures. *E. coli* treatment of co-cultures induced an 3.2-fold increase in comparison with control untreated co-cultures. Incubation of *E. coli*-treated BBEC mono-cultures with 50 μM $AACOCF_3$, 2.5 μM BEL or with COX-2-specific inhibitor NS-398 (5.0 μM) caused an inhibition of *E. coli*-induced VEGF release by 70%, 67% and 71% respectively. Incubation of untreated co-cultures with the three inhibitors decreased VEGF release by about 33% and in *E. coli*-treated co-cultures $AACOCF_3$, BEL and NS-398 caused an inhibition of VEGF release by 77%, 75% and 79% respectively. The effect of the inhibitors on VEGF release in untreated and *E. coli*-treated BRPC mono-cultures was about 22% and 21% respectively.

Table 4. VEGFA determination in BBEC and BRPC in mono- and co-culture stimulated and non-stimulated by *E. coli* K1.

		VEGFA (pg ml^{-1})	
		Control cells	Cells + *E. coli*
Mono-culture	BBEC	22.3 ± 1.9	70.4 ± 7.5*
	BBEC + $AACOCF_3$	13.5 ± 1.4[a]	21.1 ± 2.3[a]
	BBEC + BEL	16.3 ± 1.8[a]	23.2 ± 3.4[a]
	BBEC + NS-398	15.5 ± 1.7[a]	20.4 ± 2.3[a]
	BRPC	35.7 ± 3.2[b]	33.8 ± 2.9[b]
	BRPC + $AACOCF_3$	27.3 ± 2.3[a]	26.1 ± 2.5[a]
	BRPC + BEL	29.0 ± 3.1[a]	27.2 ± 3.1[a]
	BRPC + NS-398	26.8 ± 2.3[a]	26.8 ± 3.2[a]
Co-culture	BBEC/BRPC	80.7 ± 6.7[c]	260.5 ± 22.1*
	BBEC/BRPC + $AACOCF_3$	54.2 ± 4.7[a]	60.4 ± 5.3[a]
	BBEC/BRPC + BEL	56.4 ± 4.2[a]	65.1 ± 5.6[a]
	BBEC/BRPC + NS-398	50.8 ± 4.3[a]	55.2 ± 4.7[a]

a. Statistically significant differences in VEGF release of cultures incubated with inhibitors in comparison with the respective in absence of inhibitors.
b. The statistically significant differences in VEGF release in untreated BRPC mono-cultures in comparison with untreated BBEC mono-cultures.
c. The statistically significant differences in VEGF release in co-cultures in comparison with the mono-cultures.
BBEC and BRPC (40 000 cells cm^{-2}) were cultured in monolayers or were grown on the Transwell insert in 50% DMEM plus 50% F-10 HAM's containing 10% FBS. Inhibitors, 50 μM $AACOCF_3$, 2.5 μM BEL and 5 μM NS-398, were added to the culture medium 60 min before *E. coli* addition. Aliquots of medium from mono- and co-cultures in absence (control) and in presence of *E. coli* (10^7 cfu per well, for 60 min) were incubated with bovine VEGF-A antibody as described in *Experimental procedures*.
Values (means ± SEM) are from three independent experiments ($n = 3$). ANOVA and the Tukey post-test were used to compare VEGF release in the 24 different experimental conditions ($P < 0.05$).
Statistically significant differences of *E. coli*-stimulated mono- and co-cultures in comparison with not stimulated (control) cultures are indicated by asterisk (*).

These data indicate the involvement of PLA_2, AA production and its metabolization in eicosanoids in the production of PGE_2 and VEGF.

E. coli *adhere to BBEC and BRPC but only in BBEC the invasion occurs*

In Fig. 3, SEM images of BBEC, grown on the membrane of the inserts (Fig. 3A and B) and on glass cover slides (Fig. 3C and D), after 60 min of incubation with *E. coli*, show the cells with an elongated and spindle phenotype, with numerous microvilli distributed on most of the cell surface (Fig. 3A and C). The images at higher magnification show the bacteria attached to the apical surface of the BBEC in contact with microvilli (Fig. 3B and D). In Fig. 4, SEM images of BRPC, grown on the membrane of the inserts (panels A and B) and on cover slides (panels C and D) are shown. The cells are branched and flat with short microvilli on the surface area (Fig. 4A). Few bacteria were found attached to the smooth part of the BRPC surface without any sign of specific membrane action (Fig. 4B–D).

TEM of BRPC and BBEC highlights the different behaviour of the bacteria in respect to the two cell types. Figure 5A shows BRPC with numerous bacteria on the cell surface where they remain and no endocytosed bacteria were found. In *E. coli*–BBEC interaction, electron-dense bacteria both intra- and extracellular were seen (Fig. 5C). Moreover, in the presence of *E. coli,* BBEC formed microvilli-like protrusions that surrounded and endocytosed the bacteria (Fig. 5B and D). In panel D, TJ appear as points of lateral membrane fusion between the outer leaflets of adjacent endothelial cell membranes. These findings suggested that *E. coli* invasion and traversal require actin cytoskeleton rearrangements in BBEC. The results confirm data already present in literature which indicate that *E. coli* invasion of ECs occurs by a zipper-like mechanism in which the host cell plasma membrane enwraps the invading bacteria and becomes an endosome (Presadarao *et al*., 1999). This mechanism requires *E. coli* cell-induced EC cytoskeletal rearrangements for the accumulation of actin at the site of bacterial entry; it has also been demonstrated that *E. coli* K1 internalizes HBMEC via caveolae and that the scaffolding domain of caveolin-1 plays a significant role in the formation of endosomes (Sukumaran *et al*., 2002). Moreover, as we found, there is no evidence of bacterial killing inside the endosome, which could be due to the ability of bacteria within the endosome to avoid the fusion of lysosomes. No bacterial multiplication has been seen in the endosome.

VEGFR-1 is involved in E. coli *adhesion and invasion of BBEC*

Western blot analysis showed a protein level of VEGFR-1 in BRPC mono- and co-cultures 2.0-fold and 2.2-fold higher than that of BBEC in mono- and in co-cultures

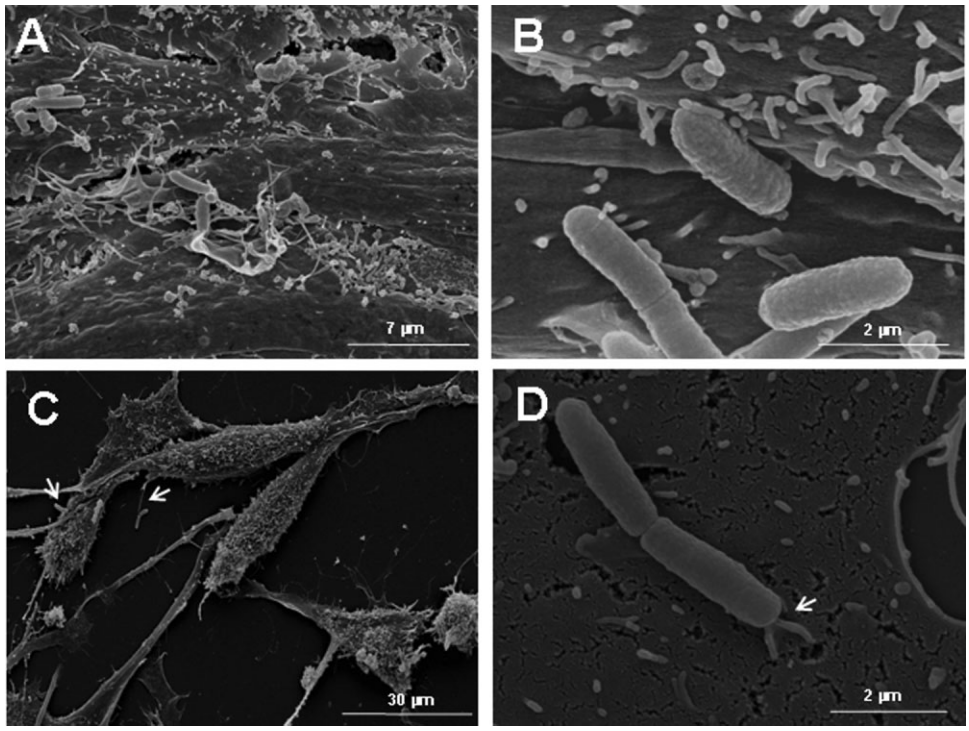

Fig. 3. SEM of BBEC on Transwell filter (A, B) and on glass coverslips (C, D) at 60 min post infection with *E. coli*.
A. Several cells on Transwell filter at lower magnification (× 4500) show an elongated and spindle phenotype with numerous microvilli distributed over the surface and bacteria adhering in contact with them.
B. Cells on Transwell filter at higher magnification (× 15 000).
C. BBECC with elongate and spindle phenotype with microvilli in contact with bacteria (white arrows) magnification, × 1100.
D. Higher magnification (× 15 000) showing the microvilli attaching to the bacteria in close and intimate contact with the bacterial surface (white arrow).

respectively (Fig. 6A). VEGFR-2 protein level remains almost unchanged in BBEC grown in contact with BRPC in respect to BBEC mono-culture. Interestingly, VEGFR-2 protein, expressed in BBEC, was not detected in BRPC (Fig. 6B). After incubation of mono- and co-cultures with *E. coli*, in presence or not of 50 µM $AACOCF_3$ or of 2.5 µM BEL, we did not find differences in receptors 1 and 2 protein amount, assessed by immunoblotting (data not shown), in comparison with non-infected cells.

With the purpose of analysing whether VEGF receptors are involved in *E. coli* K1 adhesion and invasion, assays were performed in presence of VEGFR-1 or VEGFR-2 antibodies (Ab). As shown in Fig. 6C, VEGFR-1 Ab and VEGFR-2 Ab, have no effect on *E. coli* adhesion to BBEC both in mono- and in co-cultures, as well as on *E. coli* adhesion after addition to BRPC in mono- and in co-cultures (Fig. 6D). VEGFR-1 Ab was efficient in significantly reducing *E. coli* invasion in BBEC by 30% and by 48% in mono- and in co-cultures respectively (Fig. 6E), while VEGFR-2 did not cause any change in the *E. coli* invasion of BBEC. These results indicate that the blocking of VEGFR-1 and the blocking of *E. coli* invasion are strongly correlated. Invasion of BRPC was also analysed but no intracellular bacteria have been found in any experiments performed, indicating that *E. coli* is not able to enter these cells. These results support our TEM observations: *E. coli* associate with BRPC to an extent lower than that with BBEC and it is not able to invade the PC. From these data we conclude that early association of *E. coli* with BRPC is a process separated from invasion and mediated by structures also present in the BRPC. To have the evidence that the anti-VEGFR-2 antibody was effective in the binding to its own receptor, we treated BBEC with 10 ng ml^{-1} VEGF for 15 and 30 min in absence or in presence of VEGFR-2 Ab and cell lysates were prepared for Western blotting to evaluate receptor phosphorylation (Fig. 6F). Phosphorylation of VEGFR-2 at Tyr1175 was observed in BBEC treated for 15 and 30 min with VEGF. Addition of 10 ng ml^{-1} VEGF in presence of 2 µg ml^{-1} VEGFR-2 antibody inhibited VEGFR-2 phosphorylation, demonstrating that the VEGFR-2 antibody was effective in binding the receptor and thus confirming that there is not a role for VEGFR-2 in bacterial entry into BBEC. Experiments were also performed by treating BBEC with 10 ng ml^{-1} VEGF for 15 and 30 min in absence or in presence of VEGFR-1 Ab. Phosphorylation of VEGFR-1 at Tyr1333 was observed in BBEC treated for 15 and 30 min with VEGF. Addition of 10 ng ml^{-1} VEGF

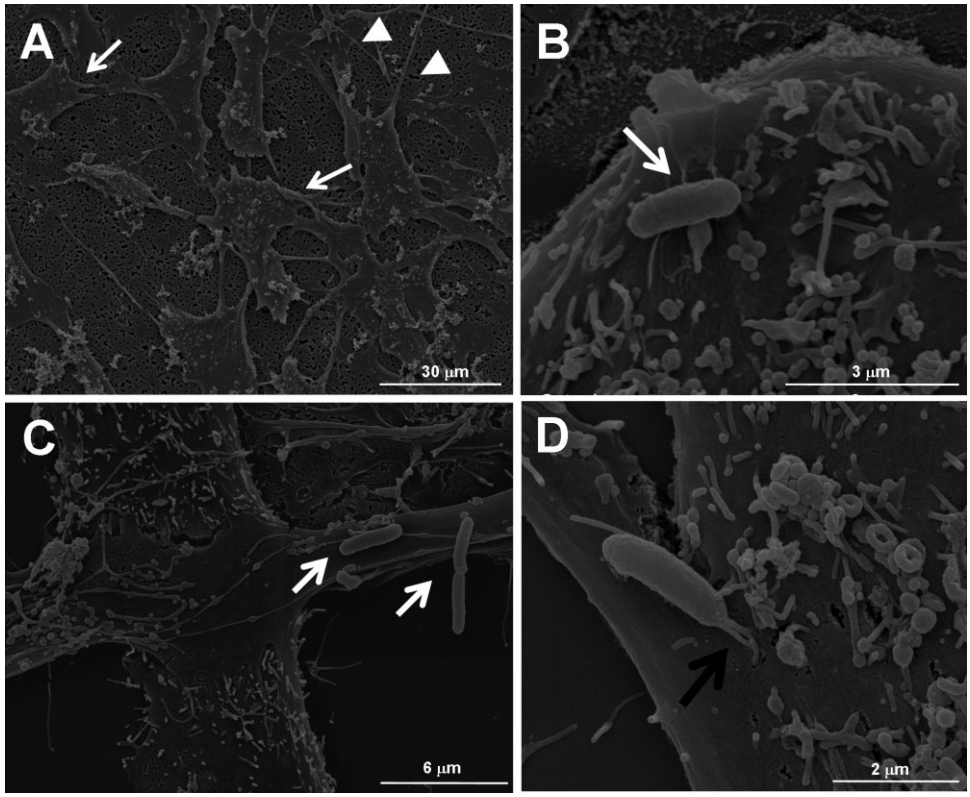

Fig. 4. SEM micrograph of BRPC at 60 min post infection with *E. coli*. (A, magnification, × 1000): the BRPC on Transwell filter exhibit a flattened shape with several branches, numerous pseudopodia (thin arrows) and filopodia (arrowheads). The bacteria were found on the cell surface, in proximity of numerous microvilli (B, magnification, × 10 000 and C, magnification, × 5000, white arrows) or, in rare cases, in contact with microvilli (D, magnification, × 15 000, black arrow).

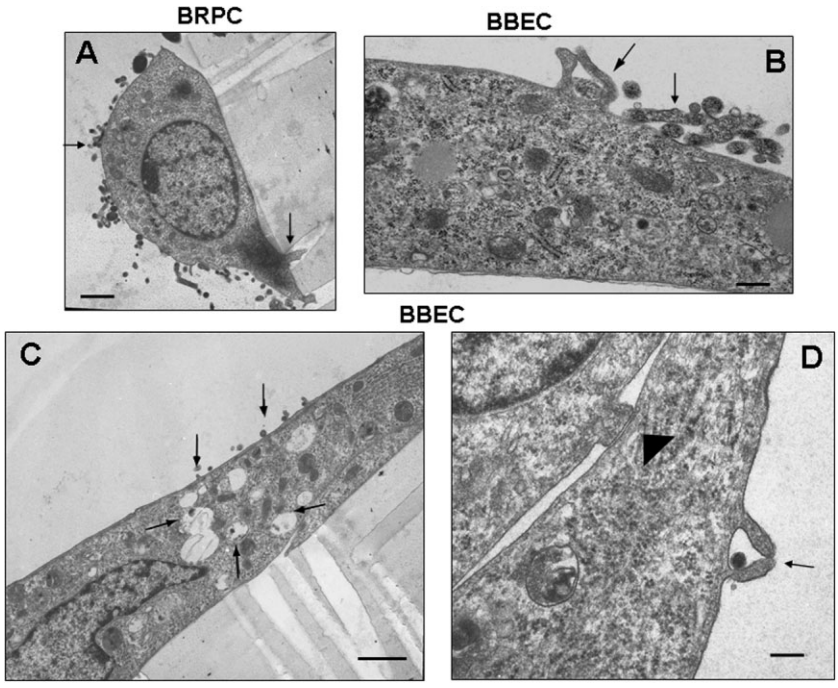

Fig. 5. Transmission electron micrographs of BRPC (A) and BBEC (B–D) infected with *E. coli* for 60 min.
A. BRPC on Transwell insert showing cellular protrusions infiltrating the filter pores (black arrow). Numerous bacteria are present on the surface (dark black) but no intracellular bacteria were found (bar = 1 μm).
B. After incubation for 60 min of BBEC with *E. coli*, electron-dense bacteria appeared to be in closely contact with endothelial cell membrane (black arrows) which encircle the microorganism (bar = 0.804 μm).
C. Electron-dense (dark black) bacteria were seen extracellularly and some bacteria were intracellularly engulfed inside membranes-bound vacuoles (thick black arrows) (bar = 1.25 μm).
D. Microvilli-like structures from BBEC form around *E. coli* (black arrow). No bacteria are seen in the paracellular space. Tight junctions are detected in neighbouring endothelial borders (arrowhead, bar = 0.33 μm).

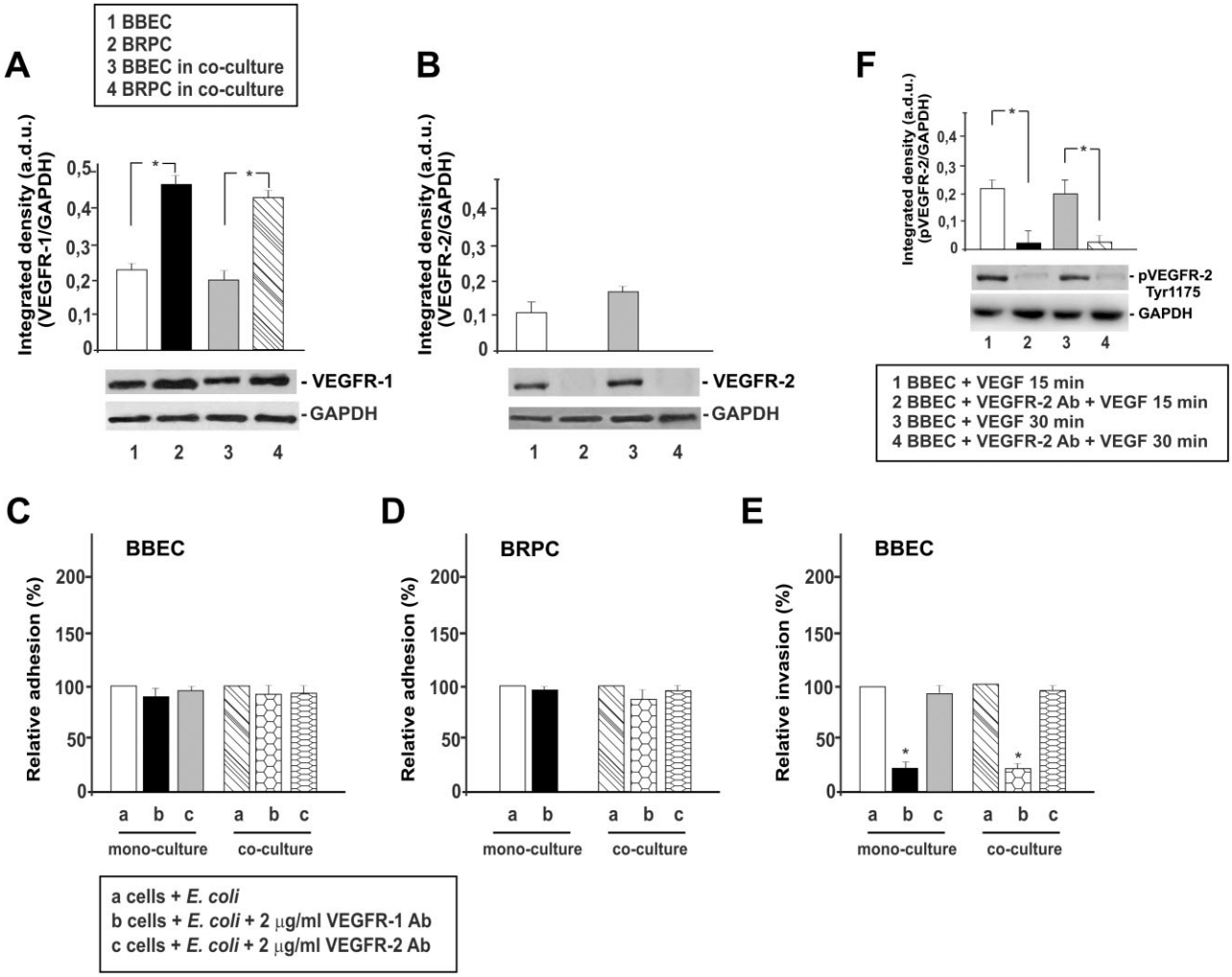

Fig. 6. Expression of VEGFR1/2, evaluated by Western blot analyses, and *E. coli* adhesion and invasion of BBEC and BRPC in mono- and in co-culture. BBEC and BRPC were grown in monolayers, lysed 60 min after *E. coli* treatment in culture, and lysates were resolved by SDS/PAGE; expressed proteins were independently revealed with mouse monoclonal antibodies against VEGFR-1 (A) and VEGFR-2 (B). All blots were controlled for equal loading by GAPDH monoclonal antibody. The ratios of band intensity, VEGFR-1/GAPDH and VEGFR-2/GAPDH are indicated. The values (bar graphs), expressed as arbitrary densitometric unit (a.d.u.), were obtained by the reading of blots using the Image J program. Representative gel analyses are shown; values represent means ± SD from three separate experiments. Statistically significant differences by pairwise Student's *t*-test are indicated by asterisks ($P < 0.05$). *E. coli* adhesion on mono- and co-culture BBEC (C) and BRPC (D) and invasion on mono- and co-culture BBEC (E), in absence or in presence of 2 μg ml^{-1} anti-VEGFR-1 or 2 μg ml^{-1} anti-VEGFR-2 antibodies, are expressed as relative percent. Expression of phospho-VEGFR-2 Tyr1175 was evaluated by Western blot analyses after treatment of BBEC with 10 ng ml^{-1} VEGF for 15 and 30 min in absence or in presence of VEGFR-2 Ab, to have the evidence that the anti-VEGFR-2 antibody was effective in the binding to its own receptor (F). Values are means ± SD of three independent experiments ($n = 3$) repeated in triplicate. Statistically significant differences, by one-way ANOVA and the Tukey post-test, are indicated by asterisk for the comparison between the invasion of BBEC mono- or co-culture infected by *E. coli* in presence of VEGFR-1 Ab versus the invasion of the respective mono- or co-cultures infected in absence of VEGFR-1 Ab ($P < 0.05$).

in presence of 2 μg ml^{-1} VEGFR-1 antibody inhibited VEGFR-1 phosphorylation, demonstrating that anti-VEGFR-1 antibody was effective in binding its own receptor (data not shown).

VEGFR-1 negatively regulates BRPC survival and its blockade protects the barrier integrity

To clarify if the prevention of the pericyte death and monolayer permeability can be attributed to VEGF blockade or simply blocking the initial stimulus (*E. coli*), experiments blocking the VEGFR-1 by its specific antibody (Ab) both in BBEC and in BRPC in co-culture or only in BBEC or only in BRPC before preparing the co-culture were carried out. Figure 7 reports cell count (A, B), TEER (C) and permeability (D) values measured after conducting the experiments of receptor blockade simultaneously on the two cell types or of receptor blockade on only one of the two cell types in co-culture. After incubation of BBEC/BRPC co-cultures with *E. coli*, TEER decreased by 64% and

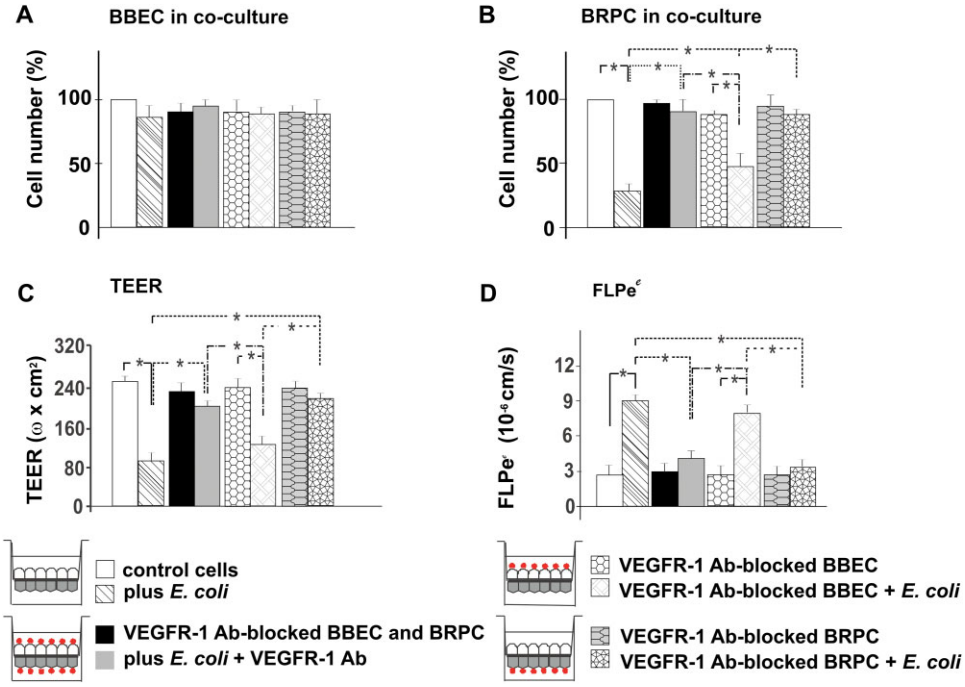

Fig. 7. VEGFR-1 blockade by specific antibody both in BBEC and in BRPC in co-culture and only in BBEC or BRPC before preparing the co-culture. BBEC/BRPC co-cultures VEGFR-1-blocked, or only BBEC VEGFR-1 blocked or only BRPC VEGFR-1 blocked before co-culture, were treated or not with *E. coli* for 60 min. Cells from inserts (0.4 μm pore size) were trypsinized separately to count BBEC and BRPC. Cell suspensions were mixed with a 0.4% (w/v) trypan blue solution, and the number of live BBEC from the co-culture with BRPC (A) and of live BRPC from the co-culture with BBEC (B) was determined using a haemocytometer. Transendothelial electrical resistance (TEER) (C) and permeability to sodium fluorescein (D) of BBEC/BRPC co-cultures VEGFR-1-blocked as above, incubated or not with *E. coli* for 60 min, were performed as described in *Experimental procedures*. Control cells refer to cells not stimulated by *E. coli*. Values are expressed as a mean ± SD of three independent experiments ($n = 3$) repeated in triplicate. Statistically significant differences, by one-way ANOVA and the Tukey post-test, are indicated by asterisk ($P < 0.05$).

permeability to sodium fluorescein increased by 3.2-fold in comparison with non-infected co-cultures (Fig. 7C and D).

Experiments with BBEC and BRPC simultaneously blocked by the VEGFR-1 Ab, confirmed that about 90% of BRPC in the co-culture remained adherent to the insert after treatment for 60 min with *E. coli*, in comparison with 30% of the BRPC adherent on the insert after the infection in the absence of receptor blockade (Fig. 7B), demonstrating that VEGFR-1 Ab significantly preserved BRPC viability by almost 3.0-fold. In this experimental condition and in presence of *E. coli*, TEER values increased by 2.3-fold and permeability decreased by about 2.2-fold in comparison with infected co-cultures in absence of receptor blockade. Moreover, only 10% of TEER reduction was observed and a 20% of increase in permeability values were found in comparison with non-infected control cells in co-culture (Fig. 7C and D).

When only the BBEC were treated with VEGFR-1 Ab, after incubation with *E. coli* for 60 min, 45% of BRPC adhering to the co-culture insert was found (Fig. 7B) unlike BBEC (Fig. 7A), whose number remained constant. In this experimental condition (BBEC blocked by VEGFR-1 Ab) a significant decrease in TEER values (about 56%) and a significant increase in permeability (approximately 2.8-fold) in *E. coli* infected in comparison with non-infected co-cultures were found. Moreover, in this experimental condition (BBEC, but not BRPC, blocked by VEGFR-1 Ab) TEER decreased by 38% and permeability increased by 2.0-fold in comparison with *E. coli* infected co-cultures in which both BBEC and BRPC were blocked by VEGFR-1 Ab (Fig. 7C and D). These results demonstrated that the VEGFR-1 blocking antibody was capable of significantly reducing *E. coli* internalization (about 50%, as demonstrated by the results reported in Fig. 6) but it has not been capable of completely abolishing the ability of *E. coli* strain to invade BBEC and to activate the signalling pathway that releases VEGF, determining the detachment of BRPC and therefore the loss of the barrier properties.

The treatment of BRPC, but not of BBEC, with VEGFR-1 blocking antibody and the subsequent *E. coli* infection, does not change the BRPC number in co-culture (Fig. 7B), whose value was very similar to that of BRPC in absence of infection. Furthermore, the values of TEER and permeability in this experimental condition

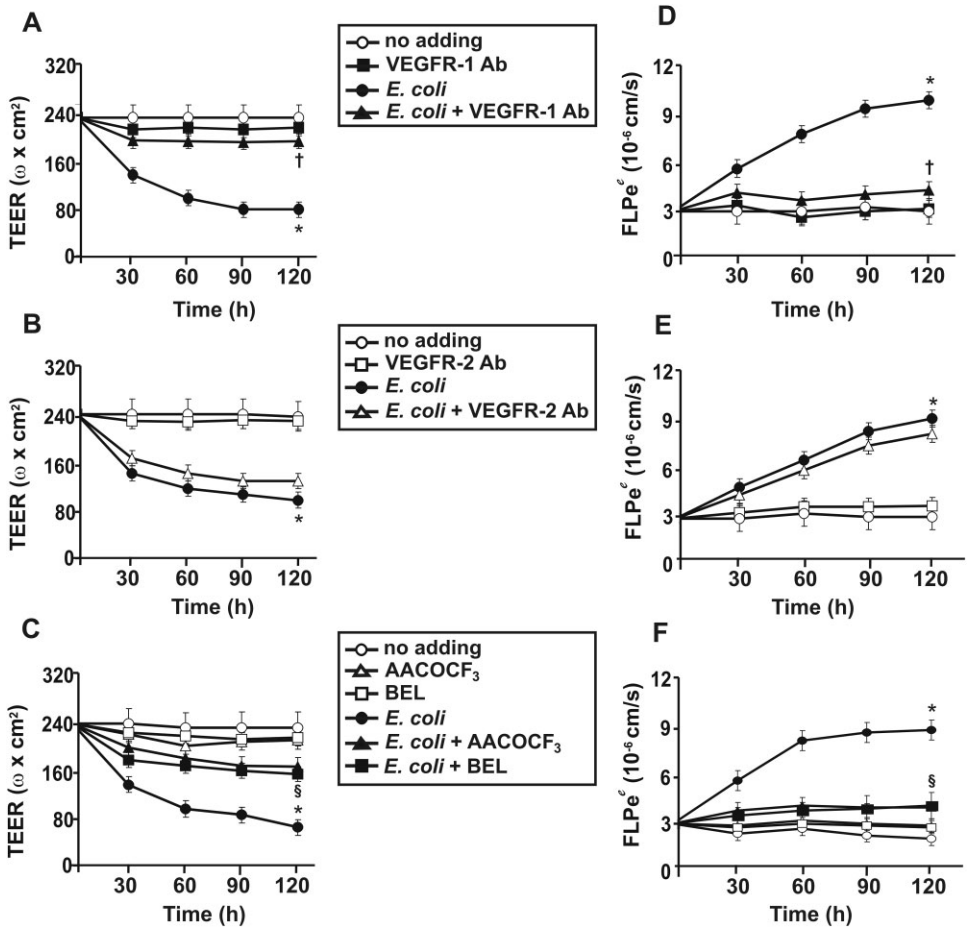

Fig. 8. Transendothelial electrical resistance (TEER) (A, B, C) and permeability to sodium fluorescein (D, E, F) of BBEC/BRPC co-culture on Transwell inserts (3.0 μm pore size) after incubation with *E. coli* K1 strain for 30, 60, 90 and 120 min in absence or in presence of 2 μg ml^{-1} VEGFR-1 or 2 μg ml^{-1} VEGFR-2 antibodies, or 50 μM $AACOCF_3$ or 2.5 μM BEL. TEER and permeability were performed as described in *Experimental procedures*. Values are expressed as a mean ± SD of three independent experiments performed in triplicate. The same time points were compared among different conditions when performing the statistical analysis. Statistically significant differences, by one-way ANOVA and the Tukey post-test ($P < 0.05$) are indicated as following: by asterisk (*), to compare stimulated *versus* control co-cultures (no adding bacteria); by dagger (†), to compare the statistically significant differences between *E. coli*-stimulated co-cultures in the presence of VEGFR-1 antibody versus the respective stimulated in the absence of VEGFR-1 antibody; by section symbol (§), to compare the statistically significant differences between *E. coli*-treated cells incubated with PLA_2 inhibitors in comparison with the respective *E. coli*-treated ones in absence of inhibitors.

were similar to non-infected control cells in co-culture. Moreover, in this experimental condition (BRPC, but not of BBEC, VEGFR-1 blocked) TEER increased by 1.7-fold and by 2.4-fold and permeability decreased by 60% and 64% in comparison with *E. coli* infected co-cultures in which only BBEC were blocked by VEGFR-1 Ab and in comparison with *E. coli* infected co-cultures in which no blocking was induced respectively (Fig. 7C and D). We postulate that, in absence of VEGFR-1 blocking antibody on BBEC, *E. coli* is able to invade BBEC without limits and therefore to activate the signalling pathway leading to VEGF production in large amounts. The VEGF released by BBEC cannot bind VEGFR-1 on BRPC, because blocked by the specific antibody, it therefore does not result in the detachment of pericytes. In this experimental condition, about 90% of BRPC adhered to co-culture and the values of TEER and permeability were very similar to those of the non-infected co-cultures.

These results demonstrate that the prevention of pericyte loss and monolayer permeability can be attributed to VEGF blockade.

To confirm our findings, we performed experiments on BBEC/BRPC co-cultures on Transwell inserts incubated with *E. coli* for 30, 60, 90 and 120 min, in absence or in presence of VEGFR-1 or VEGFR-2 Abs. As shown in Fig. 8, TEER values had already decreased after 30 min *E. coli* treatment (37% reduction) and, following incubation for 60 and 120 min, the values of TEER decreased by about 60% (panels A, B and C). The presence of VEGFR-1 Ab, but not VEGFR-2 Ab, protected the barrier

integrity, restoring TEER to values very similar to the control ones at all incubation time (panel A). No significant change were observed in the TEER values following incubation of the co-cultures with VEGFR-1 Ab and VEGFR-2 Ab in absence of *E. coli* (panels A and B). When co-cultures were infected by *E. coli* in the presence of $AACOCF_3$ or BEL, TEER was restored by about 35% at 60 and 120 min time points (panel C). Permeability studies were also performed by using fluorescein sodium to determine paracellular diffusion across BBEC/BRPC co-cultures. Fluorescent intensity in the receiver chamber had already increased of about twofold after *E. coli* incubation for 30 min (Fig. 8D–F) and the fluorescence was more intense at each designated time point than untreated co-cultures. Incubation in the presence of VEGFR-1 Ab, but not VEGFR-2 Ab, attenuated of about 2.5-fold the apical-to-basolateral diffusion of fluorescein sodium at each designated time (panels D and E). Moreover, when the cells were infected with *E. coli* for 30, 60, 90 and 120 min in the presence of $AACOCF_3$ or BEL, permeability was restored by about 44% in comparison with the values obtained when cells were infected with *E. coli* in absence of PLA_2 inhibitors (panel F). The incubation of non-infected cells with $AACOCF_3$ or BEL do not affect significantly TEER or permeability.

Discussion

Neonatal *E. coli* meningitis is associated with significant mortality and morbidity. Entry of circulating bacteria into the CNS requires the crossing of the BBB, composed of brain microvascular EC which have a dynamic interaction with other neighbouring cells, being PC, astroglia, perivascular microglia and neurones (Ballabh *et al*., 2004).

Despite the fact that the PC are morphologically situated closest to brain EC with which they share a common basement membrane, they have not been investigated in a co-culture BBB model for testing the molecular mechanism of bacterial invasion. PC communicate with EC through release of soluble factors, leading to the upregulation of BBB functions (Hori *et al*., 2004; Dohgu *et al*., 2005; 2011; Takata *et al*., 2007; Nakagawa *et al*., 2009). Recently, it has been reported that detachment of brain PC from the basal lamina occurs in disruption of the BBB caused by lipopolysaccharide-induced sepsis in mice (Nishioku *et al*., 2009) suggesting that brain PC play a crucial role in BBB integrity and cerebral microcirculation under healthy conditions. New studies have revealed that pericyte deficiency in the CNS leads to BBB breakdown and brain hypoperfusion resulting in secondary neurodegenerative changes (Winkler *et al*., 2011). Moreover, the genetic animal models of progressive PC loss with age have shown that BBB integrity is determined by the extent of PC coverage of cerebral microvessels (Bell *et al*., 2010). Loss of pericytal function can result in development of CNS disease (Bonkowski *et al*., 2011). Thus BBB dysfunction is often attributed to brain PC loss in the microvasculature.

Only a few bacteria are able to enter the brain and evoke inflammation and disease. These pathogens have developed individual strategies which allow them to adhere to and cross the brain endothelium. *E. coli* interact with endothelial receptors and enter with a zipper-like mechanism, based on direct contact of the bacterium with the endothelial cell membrane which sequentially encircles the microorganism (Presadarao *et al*., 1999), thus exhibiting brain tropism. It has been demonstrated that VEGFR-1 contributes to *E. coli* K1 invasion of human brain EC via recruitment of the PI3K/Akt signalling pathway (Zhao *et al*., 2010).

TEM and SEM images, here reported, show that *E. coli* K1 adhere to and enter BBEC, but not BRPC, by a vesicle-mediated mechanism.

In the present study, we use an *in vitro* BBB model based on co-culturing primary BBEC and BRPC on permeable Transwell inserts. This model system, showing high TEER and low permeability, indicators of barrier integrity, could be very useful for studying cell response to bacterial infection of the BBB. In this model, *E. coli* infection determines PLA_2 activation and consequently an increase in PGs synthesis. Indeed, we demonstrated that PGs are produced from BBEC in a great amount during *E. coli* infection and may play a contributory role in BBB disruption. In patients with Gram-negative bacterial infection, anti-inflammatory drugs are administered for palliative care and treatment (Kim *et al*., 2009; Hulscher *et al*., 2010). Moreover it has been reported that the elimination of PGE_2 across the BBB was inhibited by either intracerebral or intravenous administration of antibiotics, such as cefmetazole and cefazolin, and also by intracerebral administration of non-steroidal anti-inflammatory drugs (NSAIDs) such as indomethacin and ketoprofen (Akanuma *et al*., 2011). These drugs strongly inhibit human MRP4-mediated PGE_2 transport activity thereby eliminating PGE_2 across the BBB (Akanuma *et al*., 2010).

Besides, BRPC, in comparison with BBEC, release physiologically higher levels of VEGF, which may act as a stabilizing factor for BBEC. The presence of $AACOCF_3$ and BEL reduces the *E. coli*-induced VEGFA secretion of BBEC/BRPC co-cultures as well as the presence of COX-2 inhibitor NS-392, indicating the involvement of PLA_2, AA production and its metabolization in eicosanoids in the production of VEGFA. These data are in agreement with the results of other previous studies showing that in microvascular EC, PGE_2 action was associated with endothelial VEGF release and ERK2/JNK1 activation (Pai

et al., 2001) or with chemokine receptor CXCR4 upregulation (Salcedo and Oppenheim, 2003). In agreement, in other experimental systems, stimulated VEGF secretion was dependent on PLA_2 activation (Bamba *et al*., 2000; Ottino *et al*., 2004; Barnett *et al*., 2010). PGs and VEGF could exert their biological effects on BBB, probably by PC coverage ablation, thus increasing BBB permeability. In our opinion, the leakage of a certain number of pericytes is one of the mechanisms that might be strongly correlated to the loss of barrier functions. This is the first report in literature on the relationship between *E. coli* infection and microvascular PC loss. Further experiments to shed light on a possible apoptotic/necrotic process.

The fact that permeability is increased within 30 min suggests that other factors, as well as pericyte loss, may be involved in the increased permeability induced by VEGF in our model system. Certainly, VEGF plays a decisive role in the loss of function of the barrier (Murata *et al*., 1995; Hofman *et al*., 2000; 2001; Witmer *et al*., 2003), by activating specific signalling pathways that have recently also been to be activated during *E. coli* invasion of microvascular endothelial cells (Zhao *et al*., 2010). VEGF induces tyrosine kinase receptor phosphorylation, internalization and cleavage of VE-cadherin, which can cause adherens junctions to be dismantled and accompany an increase in vascular permeability (Dejana *et al*., 2008). It is well known that endothelial adherens junctions are a downstream target of VEGFR-2 signalling and it has been suggested that tyrosine phosphorylation of its components may be involved in the loosening of cell–cell contacts in established vessels to modulate transendothelial permeability (Esser *et al*., 1998).

Following *E. coli* incubation of co-cultures in which BBEC and BRPC were simultaneously blocked by the VEGFR-1 Ab or in co-cultures in which only BRPC, and not BBEC, were treated with VEGFR-1 blocking antibody, the values of TEER and permeability to sodium fluorescein were very similar to those of non-infected co-cultures. These data were confirmed by counting VEGFR-1 Ab-blocked BRPC in co-culture with BBEC without VEGFR-1 Ab-blocking after treatment with *E. coli*, suggesting that VEGFR-1 on BRPC plasma membrane negatively regulates their survival.

Moreover, after *E. coli* infection of co-cultures in presence of $AACOCF_3$ or BEL, TEER and permeability were restored by almost 40% in comparison with the values obtained when co-cultures were infected with *E. coli* in absence of PLA_2 inhibitors, demonstrating the important role played by PLA_2s in maintaining barrier properties.

The supposed events triggered by *E. coli* infection of microvascular endothelial cells are summarized in Fig. 9. The involvement of VEGFR-1 has already been shown by Zhao *et al*. (2010), which showed the colocalization of VEGFR-1 with *E. coli* during bacterial invasion of endothelial cells. In addition, they have shown the association of VEGFR-1 with the p85 subunit of phosphatidylinositol 3-kinase (PI3K) in brain microvascular endothelial cells (HBMEC) infected with *E. coli* and that *E. coli*-triggered PI3K activation in HBMEC was blocked by VEGFR-1 *si*RNA and by VEGFR inhibitors. In a previous study (Salmeri *et al*., 2012) we demonstrated that c- and $iPLA_2$ activities and $cPLA_2$ phosphorylation were stimulated in microvascular endothelial cells after *E. coli* incubation and $cPLA_2$ phosphorylation was attenuated by PI3K and ERK 1/2 inhibitors. As already shown in a previous experimental model (Barnett *et al*., 2010), we speculated that arachidonic acid released after *E. coli* infection becomes the substrate of cyclooxygenases for the production of PGs which could exert a proangiogenic influence by inducing VEGF production upon binding to target genes in endothelial cells. We think that VEGF released by endothelial cells could bind to VEGFR-1 on the membrane of adjacent pericytes and could determine their leak, acting as a negative regulator. The VEGF negative role on pericyte function was shown in the $C_3$10T1/2 pericyte line, revealing a dichotomous role for VEGF already known as a promoter of endothelial cells (Greenberg *et al*., 2008). It has also been demonstrated that the systemic delivery of VEGF ablates pericytes from the mature retinal vasculature through the VEGFR1-mediated signalling pathway, leading to increased vascular leakage and the blockade of VEGFR-1 significantly restores PC saturation in mature vessels (Cao *et al*., 2010).

Our results show the important defensive role played by the pericytes during a bacterial attack. Pericytes could be considered the cells which oversee the defence of the barrier and their survival enables the maintenance of a stronghold which opposes bacterial infection. A proper pharmacological action on the VEGFR-1, mediator of the PC detachment from the microcapillaries and on which *E. coli* develops its own 'invasive strategy' to have free access to the nervous system, would mean slowing down PC loss, thus protecting the anatomical integrity of the microvessels. The association of an antibiotic therapy with a drug able to block the VEGFR-1 on PC could represent a novel strategy to face neonatal bacterial meningitis more successfully. A better understanding of the mechanisms by which *E. coli* enter the nervous system and how they alter the communication between EC and PC may provide exciting new insight into the contribution to clinical intervention.

Experimental procedures

All reagents and antibodies were purchased from Sigma (St. Louis, MO, USA) or E. Merck (Darmstadt, Germany), unless otherwise indicated. Phospholipase A_2 inhibitors, arachidonoyl

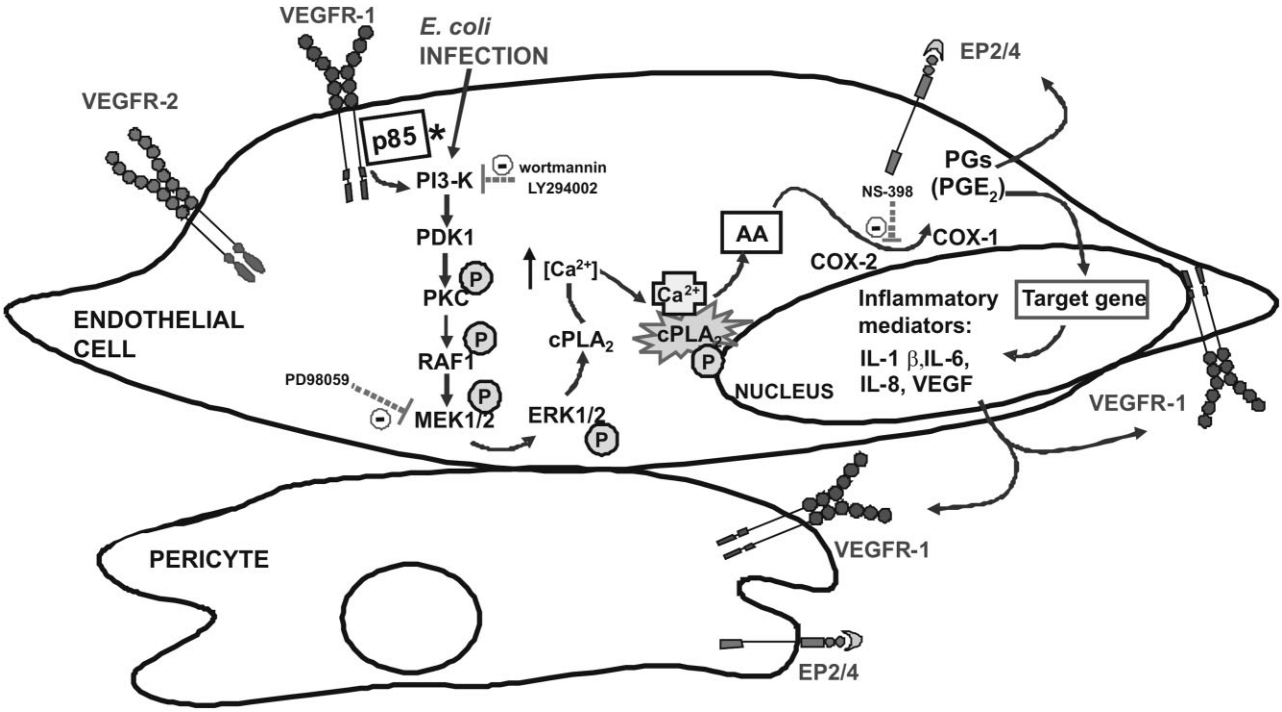

Fig. 9. A schematic model for the gene induction and lipid signalling during *E. coli* K1 infection of microvascular endothelial cells. *E. coli* K1 invasion promotes the association between phosphorylated VEGFR-1 and p85 subunit of PI3K (*Zhao *et al.*, 2010) and triggers phosphorylation of PKC-α, ERK1/2 and $cPLA_2$, via PI3K/PKD1 pathway. Arachidonic acid released becomes the substrate of cyclooxygenase for the production of PGs which could exert a proangiogenic influence by inducing VEGF synthesis upon binding to target genes in endothelial cells. VEGF released by endothelial cells could bind to VEGFR-1 on the membrane of adjacent pericytes and could determine their leak, acting as a negative regulator.

trifluoromethyl ketone ($AACOCF_3$), bromoenol lactone (BEL) and VEGF A were from Calbiochem (La Jolla, CA). NS-398 (N-[2-(cyclohexyloxy)-4-nitrophenyl]-methanesulfonamide), a selective cyclooxygenase-2 inhibitor, and rabbit polyclonal against $iPLA_2$ antibody were from Cayman Chemical (Ann Arbor, Michigan). Rabbit polyclonal against von Willebrandt factor antibody, mouse monoclonal against $cPLA_2$, VEGFR-2, α-actin and GAPDH antibodies, rabbit polyclonal against VEGFR-1 antibody, were purchased from Santa Cruz Biotechnology (CA). Rabbit polyclonal anti-phospho-VEGFR-2 Tyr1175 was from Cell Signaling Technologies and rabbit polyclonal anti-phospho-VEGFR-1 Tyr1333 was from Sigma.

A rifampicin-resistant mutant of *E. coli* K1 strain (DSMZ 10723) was used for invasion of BBEC and BRPC.

Cell cultures

Primary microvascular endothelial cells from bovine brain (BBEC) were purchased from European Collection of Cell Cultures (ECACC) and were fed with Ham's F-10 medium as previously described (Giurdanella *et al.*, 2011). Pure microvessel pericytes cultures were prepared from bovine retinas, as previously described (Lupo *et al.*, 2001). The isolated cells were then cultured in DMEM supplemented with 10% fetal bovine serum, 100 U ml^{-1} penicillin and 100 μg ml^{-1} streptomycin. Morphological changes and cell viability was determined by MTT test (Lupo *et al.*, 2002). Pericytes were characterized by their large size and branched morphology, positive immunostaining for a-smooth muscle actin, NG2 chondrotitin sulfate proteoglycan and absence of von Willebrand factor and glial fibrillary acidic protein (GFAP) staining.

Construction of in vitro *BBB model*

Inserts (Transwells, Corning, Corning, NY), were coated on the upper and bottom side with 2 mg ml^{-1} solution of rat tail collagen containing 10-fold concentrated DMEM plus 0.3 M NaOH. The coating was dried for 1 h at 37°C, and was rinsed twice with water and once with Ca^{2+}- and Mg^{2+}-free phosphate-buffered saline (PBS) before being placed in complete medium. To construct an *in vitro* model of BBB based on direct contact of cells, BRPC were first plated on the outside of the polycarbonate membrane (2×10^4 cells cm^{-2}) of the Transwell inserts (six-well type, 0.4 μm or 3.0 μm pore size), and placed upside down in the well culture plate. After BRPC have adhered, the Transwells were inverted and reinserted into six-well plates, and BBEC were seeded on the top surface of the insert (2×10^4 cells cm^{-2}) (Fig. 2). After a co-incubation for 24 h, the medium was discarded and replaced with fresh medium (50% DMEM plus 50% F-10 HAM's containing 10% FBS); under these conditions, *in vitro* BBB model was established within 3 days after cell seeding, to obtain the full confluence. As negative controls for barrier integrity studies, BBEC and BRPC in monocultures, which do not form barrier, were cultured on the inserts respectively.

Fluorescence laser scanning confocal microscopy

To characterize BBEC and BRPC in co-culture, immunocytochemistry with a confocalfluorescent microscope was performed. After incubation in co-culture, BBEC or BRPC grown on one side of the filter were removed by rubbing on filter paper to leave only one cell type. Filters with BBEC or BRPC were washed, fixed by adding 4% paraformaldehyde in PBS and processed for immunocytochemistry as previously described (Anfuso *et al*., 2007), using the following antibodies: anti-α-actin mouse monoclonal antibody, PC marker or anti-von Willebrand (vWF), rabbit polyclonal antibody, EC marker, both used to highlight cells architecture. All primary antibodies were used in a dilution 1:100. As secondary antibodies, red fluorescent-labelled CY3 and green fluorescent-labelled FITC were used in a dilution 1:1000. Distribution of immunocomplexes was observed by confocal immunofluorescence microscopy using an Olympus FV1000 confocal laser scanning microscope. Single lower power scans were followed by 16–22 serial optical sections of randomly chosen cells in four to five fields per coverslip. The average fluorescence (mean ± SD) intensity (pixel) in individual cell bodies was measured throughout the stack. Each condition was tested on a total of 60–80 cells, resulted from at least three coverslips obtained from a least two different cell cultures.

Electron microscopy

For Scanning Electron Microscopy (SEM) preparations, cells grown on the membrane were fixed with 1.5% glutaraldehyde in 0.12 M phosphate buffer (pH 7.5) overnight at 4°C. After washing with phosphate buffer several times, the membranes of the culture inserts with the cells on the two sides were removed from their support and placed into 24-well chamber slide; then were post-fixed in 1% OsO_4 for 1 h at 4°C. Following washing with distilled water, the cells on the membrane were dehydrated in graded ethanol, critical point dried and sputtered with 5 nm gold layer using an Emscope SM 300 (Emscope Laboratories, Ashford, UK) and then observed using a Hitachi S-4000 (Hitachi High-Technologies America, Schaumburg, IL) field emission scanning electron microscope.

For Transmission Electron Microscopy (TEM), after dehydrating in a graded series of acetone, cells were embedded in Durcupan ACM (Fluka Chemika-Biochemika, Buchs, Switzerland). Ultrathin sections were cut perpendicularly for the membrane using a Reichert Ultracut E microtome and double stained with uranyl acetate and lead citrate. Observations were carried out using a Hitachi H-7000 transmission electron microscope (Hitachi High-Technologies Europe GmbH, Krefeld, Germany).

Evaluation of the barrier integrity

TEER was measured using a Millicell-ERS (Millipore). The collagen-treated Transwell inserts were used to measure the background resistance. Values were expressed as $\omega \times cm^2$ and were calculated by the formula: (the average resistance of experimental wells – the average resistance of blank wells] × 0.33 (the area of the Transwell membrane).

For the determination of the flux of sodium fluorescein (Na-F) across endothelial monolayer, inserts containing cell cultures were transferred to 12-well plates containing 1.5 ml of Ringer-Hepes buffer (136 mM NaCl, 0.9 mM $CaCl_2$, 0.5 mM $MgCl_2$, 2.7 mM KCl, 1.5 mM KH_2PO_4, 10 mM NaH_2PO_4, 25 mM glucose and 10 mM Hepes, pH 7.4) in the lower or abluminal compartments. In the inserts (luminal compartment), culture medium was replaced by 0.5 ml of buffer containing 10 μg ml^{-1} Na-F (MW: 376 Da). The inserts were transferred at 5, 15 and 30 min to a new well containing Ringer-Hepes buffer. The concentrations of the marker molecule in samples from the upper and lower compartments were determined by fluorescence multiwell plate reader (PerkinElmer; excitation wavelength: 485 nm, emission wavelength: 535 nm). Flux across cell-free inserts was also measured and transendothelial permeability coefficient (Pe) was calculated. Permeability measurements of triplicate filters for each culture condition were performed. Transport was expressed as microlitres of donor (luminal) compartment volume from which the tracer is completely cleared:

$$\text{Cleared volume } (\mu l) = \text{concentration}_{\text{abluminal}} \times \text{volume}_{\text{abluminal}} \times \text{concentration}^{-1}{}_{\text{luminal}}$$

The average cleared volume was plotted versus time, and permeability × surface area product value for endothelial monolayer (PSe) was calculated by the following formula:

$$PS^{-1}{}_{\text{endothelial}} = PS^{-1}{}_{\text{total}} - PS^{-1}{}_{\text{insert}}$$

PS_e divided by the surface area (1 cm^2 for Transwell-12) generated the endothelial permeability coefficient (P_e in 10^{-6} cm s^{-1}).

Bacterial invasion and adhesion assays

Invasion of EC, in mono-culture and in co-culture with PC, by *E. coli* K1 was performed as described by Zhu *et al.* (2010b). Bacteria (10^7 cfu per well) were added to confluent cells in mono-culture or in co-culture and incubations were performed at 37°C for 60 min to allow invasion to occur. The number of intracellular bacteria was determined after incubation with gentamicin (100 μg ml^{-1}) for 1 h at 37°C. Cells were washed and lysed with 0.5% Triton X-100. The released intracellular bacteria were enumerated by seeding on LB agar plates. In duplicate experiments, the total cell-associated bacteria were determined as described for invasion, except that the gentamicin step was omitted. Results were expressed as per cent invasion [100 × (number of intracellular bacteria recovered)/(number of bacteria inoculated)].

Cell viability

In order to determine the number and the viability of BBEC and BRPC in co-culture after *E. coli* treatment for 60 min, cells from inserts were trypsinized separately, cell suspensions were mixed with a 0.4% (w/v) trypan blue solution, and the number of live cells was determined using a haemocytometer. Cells failing to exclude the dye were considered non-viable. Each infection was performed in triplicate and counted four times each.

Immunoblotting

The lysates of BBEC incubated with *E. coli* strains for 60 min were prepared for Western blotting as previously described (Giurdanella *et al*., 2011). Membranes were incubated with primary antibodies against $cPLA_2$, $iPLA_2$, VEGFR-1, VEGFR-2,

phospho-VEGFR-2 Tyr1175 or phospho-VEGFR-1 Tyr1333 and then incubated with secondary antibodies for 1 h at room temperature.

Phospholipase A_2 assay

BBEC and BRPC in mono- or in co-culture were pre-incubated for 60 min in culture medium supplemented or not with either 50 μM $AACOCF_3$ or 2.5 μM BEL. The cells were then refed with fresh culture medium containing the inhibitors in presence or in absence of *E. coli* for 60 min. Controls were performed by incubation of co-cultures with inhibitors for 120 min in absence of bacteria. At the end of the incubations, cells grown of both sides of the inserts were scraped with a rubber policeman and saved separately; BBEC and BRPC were lysed as previously described (Anfuso *et al.*, 2007) and equal amounts of cell lysates were incubated in a 96-well plate with the substrate arachidonoyl-thiophosphatidylcholine (ATPC), using $cPLA_2$ assay kit (Cayman Chemicals, Ann Arbor, MI, USA) and following the manufacturer's instructions. The use of BEL on control and bacteria-treated cells allowed us to discriminate between cytosolic and $iPLA_2$ activities. None of these components, used at the specified concentration, affected cell viability, as verified by trypan blue exclusion test. Results were expressed as pmol of ATPC hydrolysed per minute and per milligram protein (pmol min^{-1} mg^{-1}).

Determination of PGE_2 and VEGF production

To determine PGE_2 and VEGF liberation, BBEC and BRPC in mono- or in co-culture were pre-incubated for 60 min in culture medium supplemented or not with either 50 μM $AACOCF_3$ or 2.5 μM BEL or 5 μM NS-398. The cells were then re-fed with fresh culture medium containing the inhibitors in presence or in absence of *E. coli* for 60 min. Supernatants were collected and aliquots were employed for PGE_2 determination, by kit from Cayman Chemicals, Ann Arbor, MI, USA. For PGE_2, the detection range was 7.8–1000 pg ml^{-1}. Conditioned medium was removed from the mono-cultures and from the Transwells and analysed for VEGF by ELISA, using a kit from R&D Systems, Minneapolis, MN, USA, as specified by the manufacturer's instructions. For VEGF, the detection range was 20–2500 pg ml^{-1}. Each sample from three different experiments was analysed in triplicate.

VEGFR-1 blockade experiments

Experiments blocking the VEGFR-1 by its specific antibody (Ab) both in BBEC and in BRPC in co-culture and only in BBEC or BRPC before preparing the co-culture were performed.

For BBEC/BRPC simultaneous blockade experiments, co-culture were treated with 2 μg ml^{-1} VEGFR-1 Ab for 60 min before treatment with *E. coli* for 60 min. Co-cultures without VEGFR-1 blockade, were carried out in parallel.

For BBEC (but not BRPC) VEGFR-1 blockade experiments, BBEC were grown on the top surface of the Transwell insert (2×10^4 cell cm^{-2}) until confluence and then incubated with 2 μg ml^{-1} VEGR-1 Ab for 1h. BBEC were then washed three times with DPBS in order to remove as much un-attached antibody as possible, the inserts were inverted and BRPC (2×10^4 cell cm^{-2}) were seeded on the outside of the insert. After BRPC adhered, the insets were reinserted into six-well plates and co-incubated for 24 h. Then the medium was discarded, replaced by fresh medium and the *in vitro* BBB model, in which BBEC were blocked by VEGFR-1 Ab, was established within 3 days after BRPC seeding, to obtain the full confluence.

For BRPC (but not BBEC) VEGFR-1 blockade experiments, BRPC were first plated on the outside of the Transwell inserts. After BRPC adhered, the inserts were reinserted into six-well plates and BRPC were grown until confluence. BRPC were then incubated with 2 μg ml^{-1} VEGFR-1 Ab for 1 h, washed three times in order to remove as much un-attached antibody as possible and BBEC were seeded on the top surface of the insert (2×10^4 cell cm^{-2}). After a co-incubation for 24 h the medium was discarded and replaced by fresh medium and the BBB model, in which BRPC were blocked by VEGFR-1 Ab, was established within 3 days after BBEC seeding, to obtain the full confluence.

Statistical analysis

Statistical significance between two groups was analysed by Student's test. One-way analysis of variance (ANOVA), followed by Tukey's *post hoc* test, was used to compare the means for the multiple groups. The P-value < 0.05 was considered statistically significant.

Acknowledgements

With pleasure we express our gratitude to Mr. Francesco Avola for his skilled assistance; he has greatly facilitated our work as researchers contributing to achieve of many of the results here presented.

This work was supported by grants from MIUR-Italy (60% 2008/09) and PRIN 2009.

References

Akanuma, S., Hosoya, K., Ito, S., Tachikawa, M., Terasaki, T., and Ohtsuki, S. (2010) Involvement of multidrug resistance-associated protein 4 in efflux transport of prostaglandin E2 across mouse blood–brain barrier and its inhibition by intravenous administration of cephalosporins. *J Pharmacol Exp Ther* **333:** 912–919.

Akanuma, S., Uchida, Y., Ohtsuki, S., Tachikawa, M., Terasaki, T., and Hosoya, K. (2011) Attenuation of prostaglandin E2 elimination across the mouse blood–brain barrier in lipopolysaccharide-induced inflammation and additive inhibitory effect of cefmetazole. *Fluids Barriers CNS* **8:** 24.

Alberghina, M. (2010) Phospholipase A(2): new lessons from endothelial cells. *Microvasc Res* **80:** 280–285.

Anfuso, C.D., Lupo, G., Romeo, L., Giurdanella, G., Motta, C., Pascale, A., *et al.* (2007) Endothelial cell-pericyte cocultures induce PLA2 protein expression through activation of PKCalpha and the MAPK/ERK cascade. *J Lipid Res* **48:** 782–793.

Armulik, A., Genové, G., Mäe, M., Nisancioglu, M.H., Wallgard, E., Niaudet, C., *et al.* (2010) Pericytes regulate the blood–brain barrier. *Nature* **468:** 557–561.

Ballabh, P., Braun, A., and Nedergaard, M. (2004) The blood–brain barrier: an overview. Structure, regulation and clinical implications. *Neurobiol Dis* **16:** 1–13.

Bamba, H., Ota, S., Kato, A., Kawamoto, C., and Fujiwara, K. (2000) Prostaglandins up-regulate vascular endothelial growth factor production through distinct pathways in differentiated U937 cells. *Biochem Biophys Res Commun* **273:** 485–491.

Barnett, J.M., McCollum, G.W., and Penn, J.S. (2010) Role of cytosolic phospholipase A(2) in retinal neovascularization. *Invest Ophthalmol Vis Sci* **51:** 1136–1142.

Bell, R.D., Winkler, E.A., Sagare, A.P., Singh, I., LaRue, B., Deane, R., and Zlokovic, B.V. (2010) Pericytes control key neurovascular functions and neuronal phenotype in the adult brain and during brain aging. *Neuron* **68:** 409–427.

Bonkowski, D., Katyshev, V., Balabanov, R.D., Borisov, A., and Dore-Duffy, P. (2011) The CNS microvascular pericyte: pericyte-astrocyte crosstalk in the regulation of tissue survival. *Fluids Barriers CNS* **8:** 8.

Cao, R., Xue, Y., Hedlund, E.M., Zhong, Z., Tritsaris, K., Tondelli, B., *et al*. (2010) VEGFR1-mediated pericyte ablation links VEGF and PlGF to cancer-associated retinopathy. *Proc Natl Acad Sci USA* **107:** 856–861.

Dejana, E., Orsenigo, F., and Lampugnani, M.G. (2008) The role of adherens junctions and VE-cadherin in the control of vascular permeability. *J Cell Sci* **121:** 2115–2122.

Dohgu, S., Takata, F., Yamauchi, A., Nakagawa, S., Egawa, T., Naito, M., *et al*. (2005) Brain pericytes contribute to the induction and up-regulation of blood–brain barrier functions through transforming growth factor-beta production. *Brain Res* **1038:** 208–215.

Dohgu, S., Takata, F., Matsumoto, J., Oda, M., Harada, E., Watanabe, T., *et al*. (2011) Autocrine and paracrine up-regulation of blood–brain barrier function by plasminogen activator inhibitor-1. *Microvasc Res* **81:** 103–107.

Dore-Duffy, P. (2008) Pericytes: pluripotent cells of the blood brain barrier. *Curr Pharm Des* **14:** 1581–1593.

Engblom, D., Ek, M., Saha, S., Ericsson-Dahlstrand, A., Jakobsson, P.J., and Blomqvist, A. (2002) Prostaglandins as inflammatory messengers across the blood–brain barrier. *J Mol Med* **80:** 5–15.

Esser, S., Lampugnani, M.G., Corada, M., Dejana, E., and Risau, W. (1998) Vascular endothelial growth factor induces VE-cadherin tyrosine phosphorylation in endothelial cells. *J Cell Sci* **111:** 1853–1865.

van der Flier, M., Stockhammer, G., Vonk, G.J., Nikkels, P.G., van Diemen-Steenvoorde, R.A., van der Vlist, G.J., *et al*. (2001) Vascular endothelial growth factor in bacterial meningitis: detection in cerebrospinal fluid and localization in postmortem brain. *J Infect Dis* **183:** 149–153.

Giurdanella, G., Motta, C., Muriana, S., Arena, V., Anfuso, C.D., Lupo, G., and Alberghina, M. (2011) Cytosolic and calcium-independent phospholipase A_2 mediate glioma-enhanced proangiogenic activity of brain endothelial cells. *Microvasc Res* **81:** 1–17.

Gliki, G., Abu-Ghazaleh, R., Jezequel, S., Wheeler-Jones, C., and Zachary, I. (2001) Vascular endothelial growth factor-induced prostacyclin production is mediated by a protein kinase C (PKC)-dependent activation of extracellular signal-regulated protein kinases 1 and 2 involving PKC-delta and by mobilization of intracellular Ca2+. *Biochem J* **353:** 503–512.

Greenberg, J.I., Shields, D.J., Barillas, S.G., Acevedo, L.M., Murphy, E., Huang, J., *et al*. (2008) A role for VEGF as a negative regulator of pericyte function and vessel maturation. *Nature* **456:** 809–813.

Hofman, P., Blaauwgeers, H.G., Tolentino, M.J., Adamis, A.P., Nunes Cardozo, B.J., Vrensen, G.F., and Schlingemann, R.O. (2000) VEGF-A induced hyperpermeability of blood-retinal barrier endothelium *in vivo* is predominantly associated with pinocytotic vesicular transport and not with formation of fenestrations. Vascular endothelial growth factor-A. *Curr Eye Res* **21:** 637–645.

Hofman, P., van Blijswijk, B.C., Gaillard, P.J., Vrensen, G.F., and Schlingemann, R.O. (2001) Endothelial cell hypertrophy induced by vascular endothelial growth factor in the retina: new insights into the pathogenesis of capillary non-perfusion. *Arch Ophthalmol* **119:** 861–866.

Hori, S., Ohtsuki, S., Hosoya, K., Nakashima, E., and Terasaki, T. (2004) A pericyte-derived angiopoietin-1 multimeric complex induces occludin gene expression in brain capillary endothelial cells through Tie-2 activation *in vitro*. *J Neurochem* **89:** 503–513.

Hulscher, M.E., Grol, R.P., and van der Meer, J.W. (2010) Antibiotic prescribing in hospitals: a social and behavioural scientific approach. *Lancet Infect Dis* **10:** 167–175.

Kajdaniuk, D., Marek, B., Foltyn, W., and Kos-Kudła, B. (2011) Vascular endothelial growth factor (VEGF) – part 1: in physiology and pathophysiology. *Endokrynol Pol* **62:** 444–455.

Kim, K.S. (2003) Pathogenesis of bacterial meningitis: from bacteraemia to neuronal injury. *Nat Rev Neuroscience* **4:** 376–385.

Kim, K.S. (2008) Mechanisms of microbial traversal of the blood–brain barrier. *Nat Rev Microbiol* **6:** 625–634.

Kim, S.Y., Chang, Y.J., Cho, H.M., Hwang, Y.W., and Moon, Y.S. (2009) Non-steroidal antiinflammatory drugs for the common cold. *Cochrane Database Syst Rev* (3)**:** CD006362.

Kong, J.S., Yoo, S.A., Kang, J.H., Ko, W., Jeon, S., Chae, C.B., *et al*. (2011) Suppression of neovascularization and experimental arthritis by d-form of anti-flt-1 peptide conjugated with mini-PEG(™). *Angiogenesis* **14:** 431–442.

Krishnan, S., Fernandez, G.E., Sacks, D.B., and Prasadarao, N.V. (2012) IQGAP1 mediates the disruption of adherens junctions to promote *Escherichia coli* K1 invasion of brain endothelial cells. *Cell Microbiol* **14:** 1415–1433.

Lupo, G., Anfuso, C.D., Ragusa, N., Strosznajder, R.P., Walski, M., and Alberghina, M. (2001) t-Butyl hydroperoxide and oxidized low density lipoprotein enhance phospholipid hydrolysis in lipopolysaccharide-stimulated retinal pericytes. *Biochim Biophys Acta* **1531:** 143–155.

Lupo, G., Assero, G., Anfuso, C.D., Nicotra, A., Palumbo, M., Cannavò, G., *et al*. (2002) Cytosolic phospholipase A2 mediates arachidonoyl phospholipid hydrolysis in immortalized rat brain endothelial cells stimulated by oxidized LDL. *Biochim Biophys Acta* **1585:** 19–29.

Murata, T., Ishibashi, T., Khalil, A., Hata, Y., Yoshikawa, H., and Inomata, H. (1995) Vascular endothelial growth factor plays a role in hyperpermeability of diabetic retinal vessels. *Ophthalmic Res* **27:** 48–52.

Nakagawa, S., Deli, M.A., Kawaguchi, H., Shimizudani, T., Shimono, T., Kittel, A., *et al*. (2009) A new blood–brain barrier model using primary rat brain endothelial cells,

pericytes and astrocytes. *Neurochem Int* **54:** 253–263.

Nico, B., and Ribatti, D. (2012) Morphofunctional aspects of the blood–brain barrier. *Curr Drug Metab* **13:** 50–60.

Nishioku, T., Dohgu, S., Takata, F., Eto, T., Ishikawa, N., Kodama, K.B., *et al.* (2009) Detachment of brain pericytes from the basal lamina is involved in disruption of the blood–brain barrier caused by lipopolysaccharide-induced sepsis in mice. *Cell Mol Neurobiol* **29:** 309–316.

Ottino, P., Finley, J., Rojo, E., Ottlecz, A., Lambrou, G.N., Bazan, H.E., and Bazan, N.G. (2004) Hypoxia activates matrix metalloproteinase expression and the VEGF system in monkey choroid-retinal endothelial cells: involvement of cytosolic phospholipase A2 activity. *Mol Vis* **10:** 341–350.

Pai, R., Szabo, I.L., Soreghan, B.A., Atay, S., Kawanaka, H., and Tarnawski, A.S. (2001) PGE(2) stimulates VEGF expression in endothelial cells via ERK2/JNK1 signaling pathways. *Biochem Biophys Res Commun* **286:** 923–928.

Presadarao, N.V., Wass, C.A., Stins, M.F., Shimada, H., and Kim, K.S. (1999) Outer membrane protein A-promoted actin condensation of brain microvascular endothelial cells is required for *Escherichia coli* invasion. *Infect Immun* **67:** 5775–5783.

Salcedo, R., and Oppenheim, J.J. (2003) Role of chemokines in angiogenesis: CXCL12/SDF-1 and CXCR4 interaction, a key regulator of endothelial cell responses. *Microcirculation* **10:** 359–370.

Salmeri, M., Motta, C., Mastrojeni, S., Amodeo, A., Anfuso, C.D., Giurdanella, G., *et al.* (2012) Involvement of PKCα-MAPK/ERK-phospholipase A(2) pathway in the *Escherichia coli* invasion of brain microvascular endothelial cells. *Neurosci Lett* **511:** 33–37.

Sá-Pereira, I., Brites, D., and Brito, M.A. (2012) Neurovascular unit: a focus on pericytes. *Mol Neurobiol* **45:** 327–347.

Stanimirovic, D.B., and Friedman, A. (2012) Pathophysiology of the neurovascular unit: disease cause or consequence? *J Cereb Blood Flow Metab* **32:** 1207–1221.

Subramanian, J., Morgensztern, D., and Govindan, R. (2010) Vascular endothelial growth factor receptor tyrosine kinase inhibitors in non-small-cell lung cancer. *Clin Lung Cancer* **11:** 311–319.

Sukumaran, S.K., Quon, M.J., and Prasadarao, N.V. (2002) *Escherichia coli* K1 internalization via caveolae requires caveolin-1 and protein kinase Calpha interaction in human brain microvascular endothelial cells. *J Biol Chem* **277:** 50716–50724.

Takata, F., Dohgu, S., Yamauchi, A., Sumi, N., Nakagawa, S., Naito, M., *et al.* (2007) Inhibition of transforming growth factor-beta production in brain pericytes contributes to cyclosporin A-induced dysfunction of the blood–brain barrier. *Cell Mol Neurobiol* **27:** 317–328.

Wheeler-Jones, C., Abu-Ghazaleh, R., Cospedal, R., Houliston, R.A., Martin, J., and Zachary, I. (1997) Vascular endothelial growth factor stimulates prostacyclin production and activation of cytosolic phospholipase A2 in endothelial cells via p42/p44 mitogen-activated protein kinase. *FEBS Lett* **420:** 28–32.

Winkler, E.A., Bell, R.D., and Zlokovic, B.V. (2011) Central nervous system pericytes in health and disease. *Nat Neurosci* **14:** 1398–1405.

Witmer, A.N., Vrensen, G.F., Van Noorden, C.J., and Schlingemann, R.O. (2003) Vascular endothelial growth factors and angiogenesis in eye disease. *Prog Retin Eye Res* **22:** 1–29.

Zhao, W.D., Liu, W., Fang, W.G., Kim, K.S., and Chen, Y.H. (2010) Vascular endothelial growth factor receptor 1 contributes to *Escherichia coli* K1 invasion of human brain microvascular endothelial cells through the phosphatidylinositol 3-kinase/Akt signaling pathway. *Infect Immun* **78:** 4809–4816.

Zhu, L., Pearce, D., and Kim, K.S. (2010a) Prevention of *Escherichia coli* K1 penetration of the blood–brain barrier by counteracting the host cell receptor and signaling molecule involved in *E. coli* invasion of human brain microvascular endothelial cells. *Infect Immun* **78:** 3554–3559.

Zhu, L., Maruvada, R., Sapirstein, A., Malik, K.U., Peters-Golden, M., and Kim, K.S. (2010b) Arachidonic acid metabolism regulates *Escherichia coli* penetration of the blood–brain barrier. *Infect Immun* **78:** 4302–4310.